Instantaneous Speed Detection with Parameter Identification for ac Servo Systems

Kouetsu Fujita and Katsumasa Sado

Abstract—**Two methods adopting advanced control technology in order to improve the performance of ac servo systems are described in this paper. The first method is the detection of instantaneous speed using an observer. This method provides good response in speed control because it is possible to detect exactly the speed without detection dead time over a wide range of speeds. The second method is the identification of the mechanical inertia time corresponding to motor and load based on the model reference adaptive system (MRAS). This method enables the instantaneous speed detection to be applied to systems in which the mechanical inertia time is unknown. Moreover, it can realize the automatic adjustment of a speed controller using the result of identification. The effectiveness of these methods has been confirmed by experimentation. The experimental system is composed of a digital controller with a digital signal processor (DSP), a PWM inverter, and a permanent magnetic motor.**

I. Introduction

RECENTLY, a need has arisen for a servo system that incorporates a high-speed response capability with digital technology. It is because of this fact that high-speed processors called digital signal processors (DSP's), which allow high accurate computation within a short sampling time, have been developed.

Presently, a pulse encoder is the most typical speed and position sensor used for servo systems. Speed detection using the encoder is calculated by counting the number of pulses generated by the encoder and interval between them [1]. This method detects the average speed, and therefore, it causes a detection dead time. When the sampling time of the speed control becomes shorter, this dead time largely determines the upper limit of the response of the speed control. Under low-speed conditions, in particular, where the interval between the pulses is wider, detection dead time has even more influence on the response. In some servo systems, the characteristics of speed control at very low speed and stopping of the motor is very important for the position control, and it especially determines the overall system performance.

With the performance improvement of processors, complicated control theory can now be realized within a short sampling time. There are some proposals that improve characteristics of speed control systems by using such new technology for minimizing detection dead time [2], [3]. However, in the case of more complicated control requirements, a new problem is introduced: the robustness of the control system towards a change in the controlled system parameters [4].

To solve these two problems is the most important in objective designing of the high performance servo systems.

In this paper, solutions adopting two advanced control methods are presented. The first solution is to compute the instantaneous speed using a disturbance torque observer. The second solution is to identify a machine inertia time, which is a necessary parameter, using a model reference adaptive system (MRAS). As a result, speed detection free from detection dead time, even for a system with unknown or changing machine inertia time, becomes possible. Significant improvement of the performance of the servo system can be expected. Further, by using the result of identification of the machine inertia time, automatic adjustments to the speed controller can be made. It is a very useful function for users.

The following describes principles of the proposed methods, the configuration method of MRAS, the experimental system, and the results of the experiments.

II. Conventional Speed Detection

This chapter describes the conventional speed detection method and lists the associated problems.

A. Average Speed Detection

Fig. 1 shows a diagram explaining the average speed detection method. First, in this method, the interval between the encoder pulse just before the current sampling point (sampling period T_s) and the pulse just before the previous sampling point is taken as the detecting period T_d. Second, the number of pulses P within the detection period is counted. From these values, an average speed during the detection period can be calculated from (1)

Paper IPCSD 91-135, approved by the Industrial Drives Committee of the IEEE Industry Applications Society for presentation at the 1990 Industry Applications Society Annual Meeting, Seattle, WA, October 7–12. Manuscript released for publication September 6, 1991.

The authors are with the Power Electronics Department, Fuji Electric Corporate R and D Ltd., Tokyo, Japan.

IEEE Log Number 9108245.

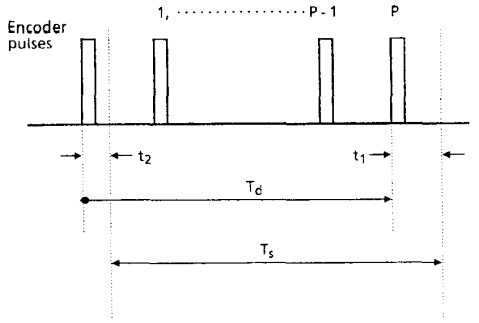

Fig. 1. Average speed detection.

and (2):

$$n = \frac{P}{T_d} \cdot K_1 \quad (\text{r/min})$$

$$= \frac{P}{T_s - t_1 + t_2} \cdot K_1 \tag{1}$$

$$k_1 = 60/P_N \tag{2}$$

where P_N is the number of encoder pulses.

The accuracy of this method depends on the frequency of the clock that counts the detection period. By making it large compared with the sampling frequency, the accuracy of speed detection is high. However, it contains a detection dead time equivalent to a half of the detection period. In particular, as Fig. 2 indicates, when the pulse interval of the encoder is longer than the sampling period and where the speed is significantly slow, the detection period becomes long, and the detection dead time increases. Consequently, stability of the speed control system greatly deteriorates.

B. One-Shot Speed Detection

This method outputs speed data immediately on receipt of the encoder pulse, which results in minimum detection dead time. It has a disadvantage, however, of limited detection range. Therefore, by changing to this method under certain speed conditions, the problem associated with the above-mentioned average speed detection method is solved.

In this method, when the speed falls below a change-over speed n_1, data corresponding to a definite speed h (r/min) is output for a certain period T_1. After the period T_1, a zero speed value is output. Fig. 3 shows this. Here, h and T_1 are decided anew in each encoder pulse interval so that the actual average value and detected average value matches. In the detected range using this method when the difference between the actual and output value h is small, the torque ripple is small. In order to make the maximum of the detected value equal to the change-over speed, h is selected as in (3). It leads to the relationship between n_1 and T_1 as shown in (4). However, in order to make up the method by software means, T_1 must be an integer multiple of the sampling period, which is shown in (5).

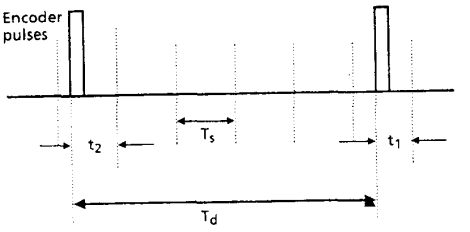

Fig. 2. Encoder pulses at very low speed.

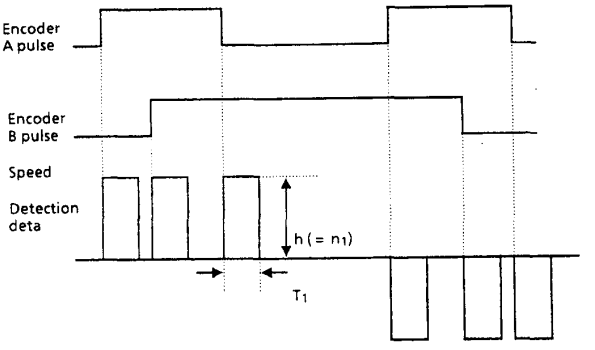

Fig. 3. One-shot speed detection.

$$h = n_1 \tag{3}$$

$$n_1 = \frac{1}{T_1} \cdot K_1 \tag{4}$$

$$T_1 = k_2 \cdot T_s \tag{5}$$

where $k_2 = 1, 2, \ldots$.

This method is called "one-shot speed detection" as it outputs a definite-width pulse, which is synchronized to the encoder pulse. Although it is free from detection dead time, this method gives rise to torque ripple under a constant speed because detected speed values look like a pulse.

Therefore, this method has a problem under steady state conditions.

III. Instantaneous Speed Detection

In order to solve the problems associated with conventional methods, which were described in section II, the principle and algorithm for the proposed instantaneous speed detection method is explained.

A. State Equation of the Control System

Fig. 4 shows a block diagram of the plant in the speed control system. The input variable here is the generated torque of the motor τ_m; state variables are the disturbance torque τ_d and instantaneous speed n; the output variable is the average speed v. Originally, the plant was the only mechanical system of the motor. However, instantaneous values for the motor speed cannot be measured directly;

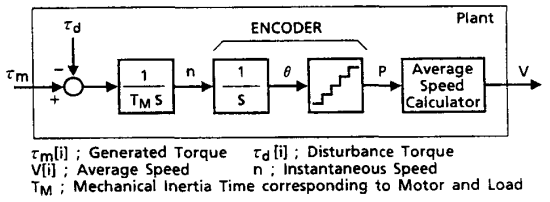

Fig. 4. Block diagram of plant.

hence, it was necessary to include the encoder and average speed calculator for control and to make the average speed an output variable, where mechanical inertia time corresponding to motor and load T_M (in seconds) is defined the necessary time that motor and load are accelerated for the maximum torque from zero to top speed.

Further, to enable all the necessary computations to be composed of the digital circuit (including the processor), the entire system is discretized. For such discretization, a virtual sampling is defined. The virtual sampling may be considered to provide sampling points for control, and they are different from the sampling points of the digital controller. Since this is one of the major characteristics of our method, it is described, and the state equations are deduced later.

The virtual sampling points proposed in this method are defined as the midpoint of the detecting period T_d, where the average speed is measured. Assuming that speed varies constantly within the detecting period T_d, the average and instantaneous speed will match at the midpoint. In other words, discretization of the system at this point allows direct measurement of the state variable and gives the instantaneous speed as an output variable. Therefore, variables of the state equation will be converted into specific values at that point and expressed by $[i]$. On the other hand, the value at the sampling point of the controller is expressed with $[i, j]$. Here, j ($j = 0, 1, 2$) stands for the number of sampling points in the measuring period of T_{di}. Fig. 5 shows the time relationship between the sampling point and virtual sampling period of each variable. At very low speeds, as shown in Fig. 6, the pulse interval of the encoder becomes larger than the sampling period, and the case $j \geq 1$ occurs. $m_i\ T_s$ in the figures indicate the time between the virtual sampling point $[i]$ and the sampling point of the controller immediately before that. The plant shown in Fig. 4 is expressed by (6)–(12).

Input variable ($U[i]$ in (6a)) becomes an average torque generated by the motor in the time T_{ai} (see (14)) between virtual sampling points, as indicated by (13). However, the generated torque of the motor is calculated from the torque constant Φ and the torque current i_T, using a straight-line approximation involving an arbitrary time t within the sampling period, as in (15).

$$X[i+1] = AX[i] + BU[i] \tag{6a}$$

$$Y[i] = CX[i] \tag{6b}$$

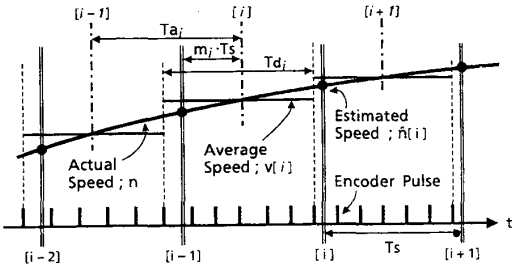

Fig. 5. Sampling points.

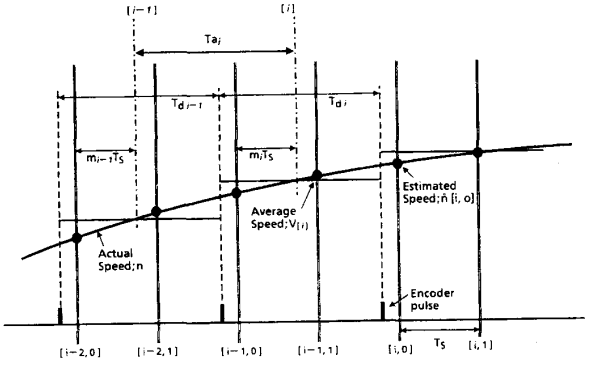

Fig. 6. Sampling points at very low speed.

where

$$d_{\tau d}(t)/dt = 0 \tag{7}$$

$$X[i] = [v[i], \tau_d[i]]^T \tag{8}$$

$$Y[i] = v[i] \tag{9}$$

$$\mathbf{A} = \begin{bmatrix} 1 & -T_{ai}/T_M \\ 0 & 1 \end{bmatrix} \tag{10}$$

$$\mathbf{B} = \begin{bmatrix} T_{ai}/T_M \\ 0 \end{bmatrix} \tag{11}$$

$$\mathbf{C} = [1 \quad 0] \tag{12}$$

$$U[i] = \Phi/T_{ai}\int_0^{Ta_i} i_T(t)\,dt = \Phi/T_{ai}\int_{m_iTs}^{m_{i+1}Ts} i_T(t)\,dt \tag{13}$$

$$T_{ai} = T_{di}/2 + T_{d+1}/2 \tag{14}$$

$$i_T(t) = i_T[i](1 - t/Ts) + i_T[i+1]t/Ts. \tag{15}$$

B. Configuration of Disturbance Torque Observer and Instantaneous Speed Calculation

Equation (6) is observable and, therefore, can be configured with the observer. Furthermore, as explained in the last section, the system can be discretized at the virtual sampling point, which allows the instantaneous

speed to be directly detected. By using the minimal-order observer of Gopinath in the discrete-time system, the disturbance torque can be estimated from (16)–(19). [5] Typically, l_i in the equation is a constant; however, here, it becomes a variable as T_{ai}, which is the sampling period of the state equation, is also a variable. The "pole" occurring in (18) is a pole for the observer that must satisfy (19) in the discrete-time system.

This method uses the instantaneous speed at the virtual sampling point to solve the equations. With the actual speed controller, however, instantaneous speed at the virtual sampling point is unknown. Therefore, the assumption is made that the disturbance torque does not change between the virtual sampling point and the current time. The detected average speed is used as an initial condition value, and the instantaneous speed is calculated from (20), using the estimated torque and electric torque current value.

Hence, (20) can be solved when the current is approximated by a straight line as in (15). For example, instantaneous speed, at current sampling point $[i, 0]$ shown in Fig. 6, is calculated from (21). Fig. 7 shows a block diagram of instantaneous speed detection.

$$\hat{Z}[i+1] = \hat{Z}[i] + l_i \cdot Ta_i/T_M \cdot (\hat{\tau}_d[i] - U[i]) \quad (16)$$

$$\hat{\tau}_d[i] = \hat{Z}[i] + l_i \cdot V[i] \quad (17)$$

where

$$l_i = (\text{pole} - 1)T_M/Ta_i \quad (18)$$

$$|\text{pole}| < 1 \quad (19)$$

$$\hat{n}[i,j] = V[i] + 1/T_M \int_{m_i Ts}^{Ts} (\Phi i_T(t) - \hat{\tau}_d(t))\, dt + 1/T_M \sum_{k=1}^{bi} \int_0^{Ts} (\Phi i_T(t) - \hat{\tau}_d(t))\, dt \quad (20)$$

$$\begin{aligned}\hat{n}[i,0] &= v[i] - Ts/T_M[(1-m_i)+1]\hat{\tau}_d[i] \\ &\quad + \Phi \cdot Ts/T_M[(1-m_i) \\ &\quad \cdot\{i_T[i-1,0](1-m_i) + i_T[i-1,1](1+m_i)\}/2 \\ &\quad + \{i_T[i-1,1] + i_T[i,0]\}/2] \end{aligned} \quad (21)$$

where bi is the number of sampling points between virtual point $[i]$ and current sampling point $[i, j]$.

$$\hat{Z}[i+1] = \hat{A}\hat{Z}[i] + \hat{B}y[i] + \hat{J}U[i]) \quad (22)$$

$$\hat{X}[i] = \hat{C}\hat{Z}[i] + \hat{D}y[i] \quad (23)$$

where

$$\hat{A} = a_{11} - l_i a_{12} = 1 + (T_{ai}/T_M) \quad (24)$$

$$\hat{B} = a_{21} - l_i a_{11} + \hat{A}l_i = l_i^2(T_{ai}/T_M) \quad (25)$$

$$\hat{C} = 1 \quad (26)$$

$$\hat{D} = l_i \quad (27)$$

$$\hat{J} = b_2 - l_i b_1 = -l_i(T_{ai}/T_M) \quad (28)$$

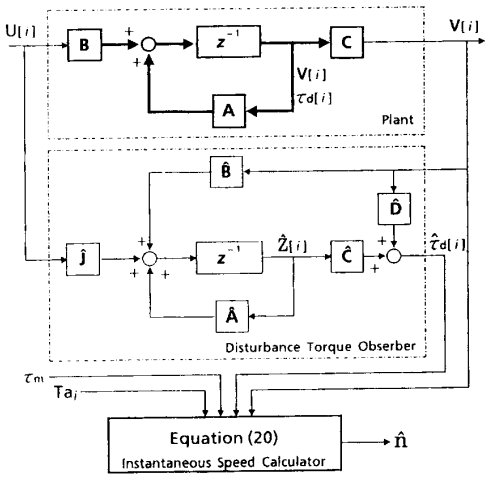

Fig. 7. Block diagram of instantaneous speed detection.

where $a_{11}, a_{12}, \cdots, b_2$ are elements of matrix A and B in (10) and (11), and where $\hat{A}$, $\hat{B}$, $\hat{C}$, $\hat{D}$, and $\hat{J}$ are constant matrixes of the minimal-order observer of Gopinath in the discrete-time system as in (22)–(28).

IV. Result of Experimentation

A. Experimental System

By using the experimental system shown in Fig. 8, evaluation on the actual machine was performed. Table I shows specifications of this system. In order to obtain a fast response, the current-control system is configured with an analog circuit, whereas the other controls are realized by DSP software. The motor has a 2000-PPR encoder and a rigidly coupled load. A disturbance-torque observer and instantaneous-speed calculator are also implemented, as shown in the block diagram in Fig. 7. In the experiment, torque generated by the motor is calculated by using the torque current reference value. This eliminates the need for inputting actual current values into the DSP so that the A/D converter is required. Therefore, this system is inexpensive. However, in order to have a more accurate estimation of the disturbance torque, the lag time of the current-control loop is taken into account during the calculation.

Although the lower detection threshold is not theoretically necessary, it is provided when the pulse of the encoder becomes too long compared with the sampling period and where the DSP execution time becomes too long and the memory use excessive. In this system, instantaneous speed is detected down to 1.5 r/min. It is one sixteenth of the speed (25 r/min) where the encoder pulse interval and sampling period match. At lower than 1.5 r/min, it changes to one-shot speed detection. In this case, torque ripple in the steady state is very small because change-over speed is exceedingly low. The maximum value of the execution time for the instantaneous speed detection part is approximately 100 μs.

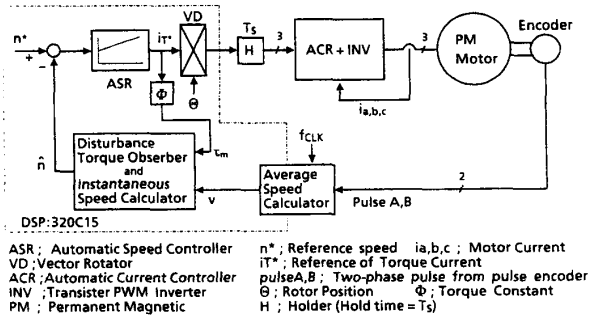

Fig. 8. System diagram.

TABLE I
CONTROLLER AND MOTOR SPECIFICATIONS

Controller	
Sampling period *Ts*	400 μs
Time resolution of *Td* ($1/f_{CLK}$)	200 ns
PWM frequency of Transistor INV.	3 kHz
Motor	
Number of poles	six poles
Power	800 W
Mechanical inertia time (with Load)	27 ms
Number of encoder pulses	2000 PPR

B. Experimental Result

In the experiment, characteristic comparison at very low speeds was made, using each of the three methods listed in Table II to provide a speed feedback value. The PI constant of the speed controller was defined so that middle- and high-speed response of the motor was most appropriate for each method. Figs. 9–11 show the result of the experiment for the three methods of Table II in these three figures, (a) is the step response, and (b) is the waveform under steady-state conditions. The waveforms show the speed detection value, direct current tachometer output for actual speed monitoring, and the *A* and *B* pulses of the encoder.

In the average speed detection in Fig. 9, hunting occurs during the transition period due to large detection dead time. Even under steady-state conditions, a disturbance triggers oscillation every once in a while. Fig. 10, which illustrates one-shot detection, shows no hunting at the transition although the overshoot is rather large.

However, under steady-state conditions, the rotation ripple is caused by the detection ripple. Instantaneous speed detection in Fig. 11 shows adequate characteristics both under steady-state and transitional conditions.

It has the following characteristics:

1) At the virtual sampling point, the state equations of the discrete system are handled. Therefore, the disturbance torque observer can be configured with minimal-order observer, allowing easier design.
2) In order to optimize CPU execution time and memory use, a lower detection threshold is set, below which one-shot detection is used.
3) Necessary signals are encoder pulses and torque current reference values, which are both available from Digital Equipment.

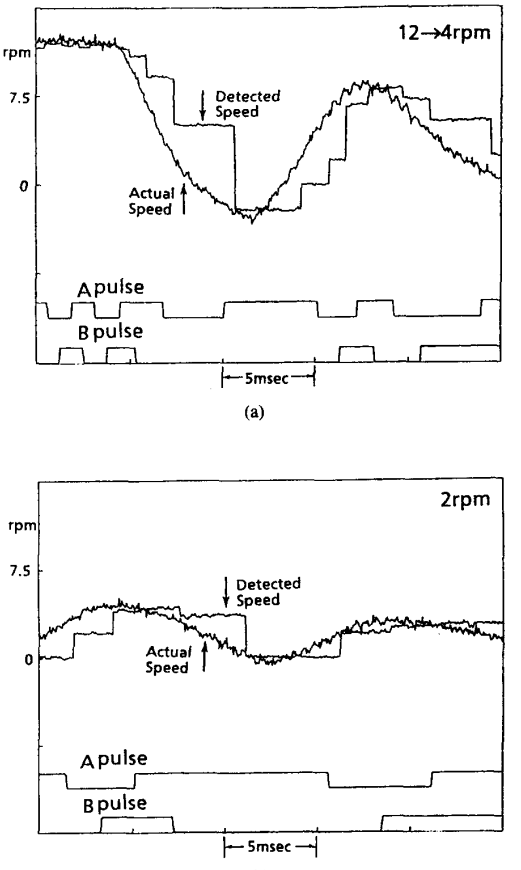

Fig. 9. Experimental result of speed control using average detection: (a) Step response; (b) steady state.

TABLE II
THREE METHODS OF SPEED DETECTION

	Detection method	Sampling period
i	Average detection	300 μsec.
ii	One-shot detection	300 μsec.
iii	Instantaneous detection	400 μsec.

The advantages gained by using this method are the following:

a) Improved characteristics of the speed controller obtained only from additional software. With this method, quality of speed response equivalent to middle to high speed can be obtained even for very low speeds. In addition, steady-state detection ripple is minimal.
b) It has the potential of reducing the equipment cost because no deterioration of performance is expected even when the number of encoder pulses is decreased.

The result, which is shown in Fig. 11, was obtained by

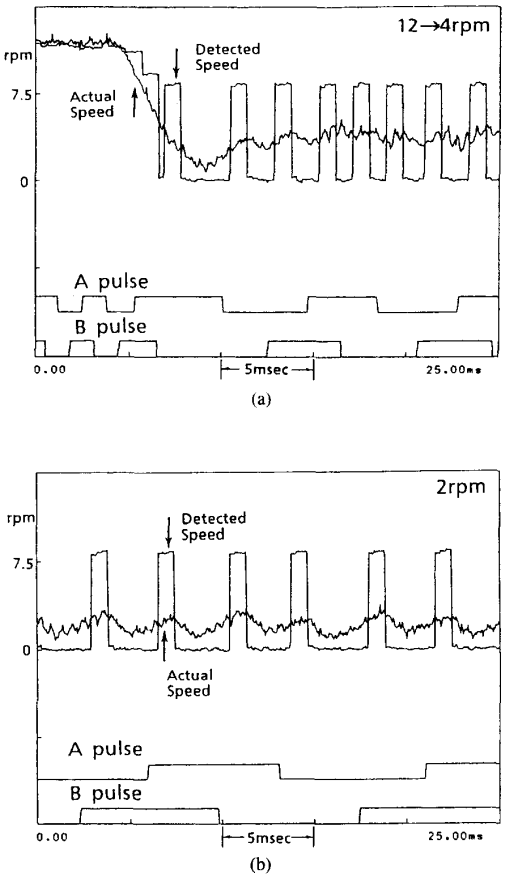

Fig. 10. Experimental result of speed control using on-shot detection: (a) Step response; (b) steady state.

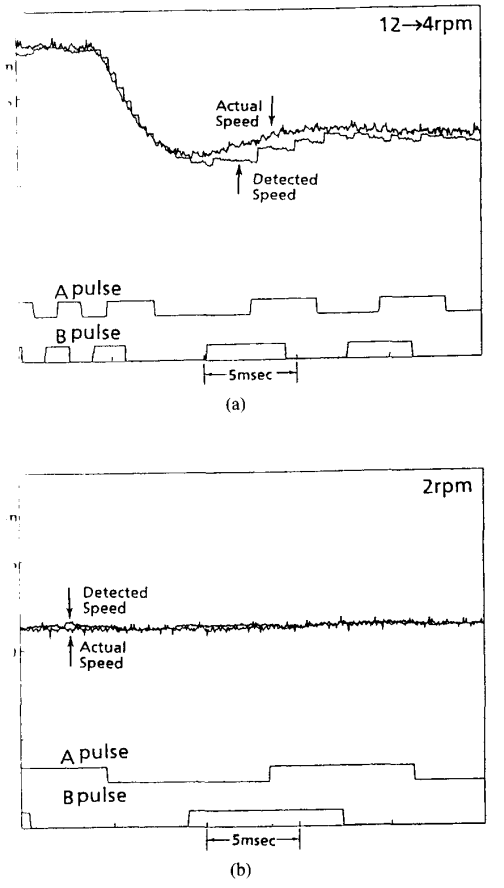

Fig. 11. Experimental result of speed control using instantaneous detection: (a) Step response; (b) steady state.

the use of actual values of the machine parameter (mechanical inertia time) in the computation of the disturbance torque observer and instantaneous speed. The instantaneous speed at every sampling point of the digital controller is given to add the speed change between the virtual sampling points and the present sampling point to the average speed measured with very high accuracy. Although the estimated error of speed caused by parameter error is not accumulated in this calculation at the middle- and high-speed ranges, it gradually becomes big at very low speeds as no encoder pulse is inputted during the sampling period. However, the accumulated errors disappear when a new encoder pulse is inputted and new virtual sampling point is defined. Therefore, the estimated error of speed until the rotor position of the servo motor does not change only one pulse is not noticed. On the other hand, the observer gain cannot be adjusted to be the most suitable in systems where mechanical inertia time is unknown or varies. In order to allow its use in such systems, an identification function for mechanical inertia time is added.

V. Identification of Mechanical Inertia Time by MRAS

A. Design of MRAS

From (6)–(12), the relationship between the generated torque of the motor and average speed is shown the difference equation (29). Generally, when parameter identification is performed, all other variables are required to be known. However, the plant contains a disturbance torque. Now, in order to identify the parameter used in the disturbance torque observer, the disturbance torque observer's estimated values cannot be used in an identification. This paper, therefore, introduces a method of canceling the disturbance torque.

First of all, (30) is assumed with regard to the disturbance torque. This equation implies that any rapid change of the disturbance torque is not expected. In a servo system that requires a fast response, sampling periods tend to be shorter, and thus, this assumption is reasonable. Then, the difference between (29) and the preceding one is found by subtraction. Using (30) leads to (31),

which does not include the disturbance torque. Consider this as the difference equation of the reference mode. MRAS is designed by using Landau's discrete time-recursive parameter identification; the result will be (32)–(35) [6], [7]. Here, (32) is the difference equation for an adjustable system (34) for a linear compensator and (35) for a adaptation mechanism. In the experiment, (34) is solved by using the value $r = 0$. Fig. 12 shows a block diagram for MRAS in such a case:

$$n[i] = n[i-1] + \frac{Ts}{T_M}(\tau_m[i-1] - \tau_d[i-1]) \quad (29)$$

$$\tau_d[i-1] = \tau_d[i-2] \quad (30)$$

$$y_M[i] = 2y_M[i-1] - y_M[i-2] + b_1 U'[i-1] \quad (31)$$

$$y^0[i] = 2y_M[i-1] - y_M[i-2] + \hat{b}_1[i-1]U'[i-1] \quad (32)$$

where

$$y_M[i] = n[i], \qquad b_1 = Ts/T_M,$$
$$U'[i-1] = \tau_m[i-1] - \tau_m[i-2]$$

$$\epsilon^0[i] = y_M[i] - y^0[i] \quad (33)$$

$$\nu^0[i] = \epsilon^0[i] + \sum_{k=0}^{r} C_k \epsilon[i-k] \quad (34)$$

$$\hat{b}_1[i] = \hat{b}_1[i-1] + \beta \frac{U'[i-1]}{1 + \beta U'[i-1]^2} \nu^0[i] \quad (35)$$

where $y^0[i]$ is calculated as the estimated speed using the previous value of identified parameter $b[i-1]$, in the adjustable system.

B. Result of Experiment

The experiment was performed by using the MRAS techniques of Fig. 12 on the system in Fig. 8. The identification computation was executed only at middle and high speeds and not at very low speeds since the execution time for instantaneous detection becomes longer at the very low speed. As a result, in spite of the fact that the execution time of MRAS was approximately 80 μs, the system could be configured without increasing the sampling time.

Fig. 13 shows the results of the identification of parameter b_1, which corresponds to the mechanical inertia time. Here, an initial value of an adjustable system's b_1 was set at twice the nominal value (i.e., half the mechanical inertia time). While the motor stepped between 500 and 1000 r/min, as shown, identification was completed after two cycles. Fig. 14 is an expanded view of Fig. 13, where the time scale of the dotted ring is enlarged. From this figure, it becomes clear that the identification value changes when the motor starts acceleration. This is because the reference model uses differentiation for cancellation of the disturbance torque. Therefore, the identification values vary most when the rate of change of torque generated by the motor and, hence, acceleration is large.

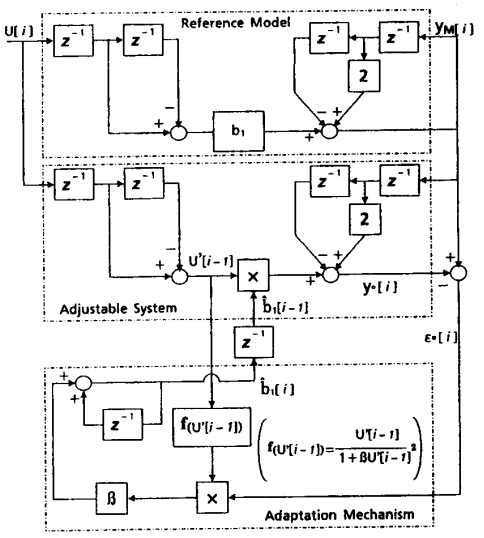

Fig. 12. Block diagram of MRA's.

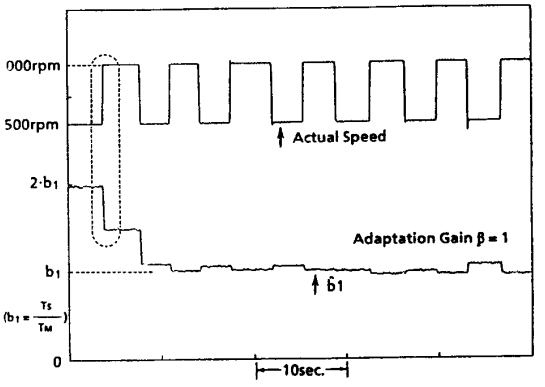

Fig. 13. Experimental result of the identification.

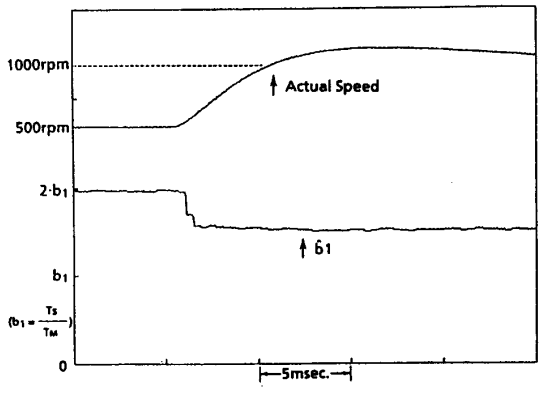

Fig. 14. Experimental time view of Fig. 11.

Although the system allows on-line identification, if the identification value changes quickly, there may be need for a large-amplitude torque current to be rapidly changed. However, it is often restricted by the application. It is, therefore, appropriate for feeding controllers of general machines and machine tools where the mechanical inertia time does not change radically.

C. Automatic Adjustment

When a speed controller is configured with PI control, design cannot be carried out unless this $P1$ constant is known. Therefore, when the mechanical inertia time is unknown or varies, the PI constant cannot be set at the most appropriate value without repeated measurements. Here, the mechanical inertia time including the load is identified so that automatic adjustment of the speed controller is possible by using the identified value. Equation (36) shows the transfer function of the PI controller used in the experiment.

$$G(S) = Kp\left(1 + \frac{1}{ST_i}\right) \tag{36}$$

where Kp is the proportional gain, and T_i is the integral time.

In the equation, by varying the proportional gain Kp in proportion to the mechanical inertia time, speed response remains constant, regardless of the mechanical inertia time. Fig. 15 shows a block diagram for the experimental system that incorporates the system proposed in this paper. This system has a sampling period T_S of 400 μs, and the speed response is 1000 rad/s or more. The filter at the output of the identifier is needed to reduce the effect of a large influence on the speed controller when the identification value changes radically.

Figs. 16 and 17 show the result of experimentation with automatic adjustment of the speed controller in this system. Conditions for the experiment are the same as in Fig. 13, where the mechanical inertia time is initially set at a half of its nominal value, and the step response is shown. When the mechanical inertia time is small, the response is not fast because the ASR gain is also small. After adjustment is made using the identification value, the ASR gain becomes large, and a good response is obtained.

VI. Conclusion

This paper proposed methods to improve performance of a servo system using two advanced control techniques. Their validity and effectiveness were confirmed by experimentation.

The first method was the instantaneous speed detection method, which uses an observer. It calculates the instantaneous speed at the time of sampling from the estimated value of the disturbance torque by using a disturbance torque observer and torque current reference values.

The second method was the identification of the mechanical inertia time by using MRAS. With instantaneous speed detection, knowledge of a mechanical inertia time

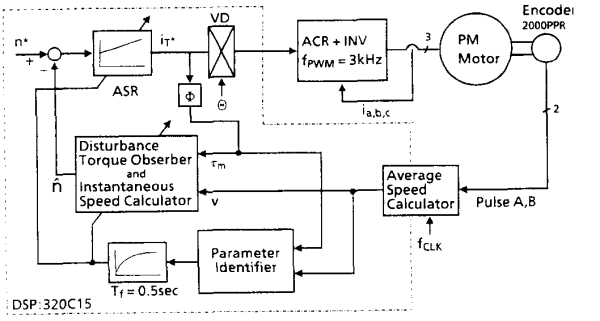

Fig. 15. Total system diagram of experiment.

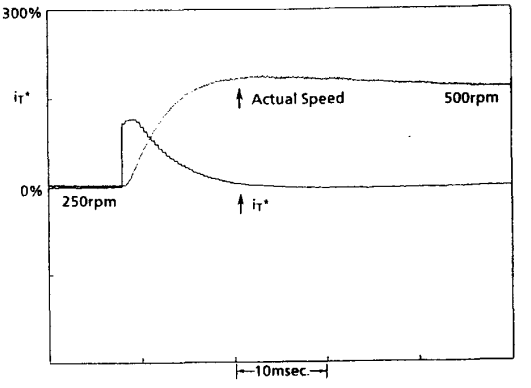

Fig. 16. Step response without automatic adjustment of ASR gain.

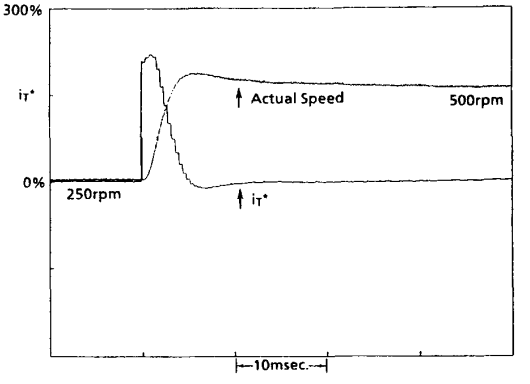

Fig. 17. Step response with automatic adjustment of ASR gain.

becomes necessary; when this value is unknown or changing, the method cannot be applied. To solve such a problem, a function to identify the mechanical inertia time is needed. This system is characterized by its unique calculation method for canceling the disturbance torque. This method is useful for a servo system that has very large frictional torque.

Then, automatic adjustment of the speed controller was performed by using the identified value. This can significantly save the adjustment time of a combined servo

system and load. Furthermore, if the mechanical inertia time changes, the same level of speed response can be obtained.

Both of the methods proposed in this paper improve the performance of the servo system in a practical manner. These methods are expected to be widely used in the future.

REFERENCES

[1] T. Ohmae *et al.*, "A microprocessor-controlled high-accuracy wide-range speed regulator for motor drives," *IEEE Trans. Ind. Electron.*, vol. IE-29, no. 3, Aug. 1982.

[2] M. Watanabe *et al.*, "Digital servo system using speed estimation observer," *T. IEE Japan*, vol. 107-D, no. 12, 1987.

[3] R. D. Lorenz *et al.*, "High resolution velocity estimation for all digital ac servo drives," in *Conf. Rec. IEEE/IAS Ann. Mtg.*, 1988, pp. 363–368.

[4] B. Courtiol *et al.*, "High speed adaptive system for controlled electrical drives," *Automatica*, vol. 11, pp. 119–127.

[5] B. Gopinath, "On the control of linear multiple input-output systems," *Bell Syst. Tech. J.*, vol. 50, no. 3, pp. 1063–1081, 1972.

[6] I. D. Landau *et al.*, *Theory & Practice of Adaptive Control System*. Tokyo: Ohm, 1981.

[7] C. Ohsawa *et al.*, "Parameter identification of 2-mass system and suppression of torsional vibration," in *Proc. IPEC-Tokyo*, 1990, pp. 428–435.

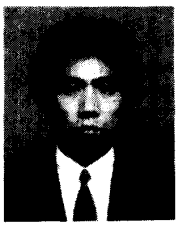

Kouetsu Fujita was born in Niigata, Japan, in 1958. He received the B.S. and M.S. degrees in electrical engineering from Nagaoka University of Technology, Niigata, Japan, in 1981 and 1983, respectively.

He joined Fuji Electric Corporate Research and Development, Ltd., Tokyo, Japan, where he is engaged in the research and development of ac motor drives in the Power Electronics Department.

Mr. Fujita is a member of the IEE of Japan.

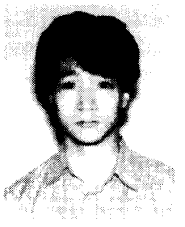

Katsumasa Sado was born in Tokyo, Japan, in 1964. He received the B.S. degree in electrical engineering from Tokyo Metropolitan University, Tokyo, Japan, in 1988.

He is with Fuji Electric Corporate Research and Development, Ltd., Tokyo, Japan, where he is engaged in the research and development of ac motor drives in the Power Electronics Department.